UDK 621.315.592

XXVII International Symposium „Nanophysics and Nanoelectronics“, Nizhny Novgorod, March 13–16 March 2023

Charged vacancies formation in AlAs anionic sublattice

© *T.S. Shamirzaev*[1,2]

[1] Rzhanov Institute of Semiconductor Physics, Siberian Branch, Russian Academy of Sciences, 630090 Novosibirsk, Russia
[2] Novosibirsk State University, 630090 Novosibirsk, Russia

E-mail: sha_tim@mail.ru

Received May 5, 2023
Revised May 18, 2023
Accepted May 18, 2023

The vacancy formation dynamics in doped semiconductor heterostructures with quantum dots (QDs) formed in the AlAs anionic sublattice has been studied. A theoretical model that describes the effect of doping on the vacancy generation dynamics is constructed. It is shown that the generation of positively charged arsenic vacancies is more probable than the generation of neutral ones at high hole concentrations. On the other hand, at high electron concentrations, the formation of neutral arsenic vacancies is more efficient than that positively charged ones. It has been experimentally revealed that the vacancy-stimulated high-temperature diffusion of antimony is enhanced (suppressed) in *p*-(*n*-)doped heterostructures with Al(Sb,As)/AlAs QDs.

Keywords: charged vacancies, quantum dots, atomic diffusion.

DOI: 10.61011/SC.2023.04.56417.01k

1. Introduction

The intrinsic point defects — vacancies have a strong influence on the electronic and atomic subsystems of semiconductor materials [1]. In structures with quantum wells (QWs) and quantum dots (QDs), the formation of vacancies at high temperatures leads to vacancy-stimulated inter-diffusion of the materials [2,3] constituting the heterostructure. Material mixing has been widely used to modify the parameters of structures, allowing to change the band gap width [4,5], control the hyperfine interaction [6], and reduce strain gradients [7]. In indirect band gap heterostructures with QW and QD formed based on the wide-band semiconductor AlAs [8,9], diffusion blurring of the hetero-boundary makes it possible to controllably change the lifetime of radiative recombination of excitons by several orders of magnitude [10].

It is well known, that vacancies in semiconductors can be electrically charged [11]. The result is a strong dependence of the vacancy formation energy on the concentration of charge carriers [12–14]. The formation of charged vacancies has been well studied in GaAs [15–17] based heterostructures. However, in AlAs, which is quite widely used to create various semiconductor devices [18,19], the formation of vacancies is much less studied.

This paper studied the dynamics of the formation of vacancies in the anionic sublattice of bulk AlAs (V_{As}) being in different charge states. It is shown that in *n*-doped AlAs, mainly uncharged vacancies are formed, while in *p*-doped material, the formation of positively charged vacancies dominates. These conclusions have been experimentally confirmed. It is found that at high temperatures diffusion-stimulated diffusion of Al(Sb,As) QDs formed in the anionic sublattice of AlAs takes place in *p*-doped and is absent in *n*-doped heterostructures.

2. Results and discussion

2.1. Theoretical model and computer modelling

The main ways of vacancies formation in a crystal are their generation on the surface (Schottky defect formation) and in the volume (Frenkel pair formation). In the first case, the surface condition (e.g., the type and structure of the coating [20–22]) and the exchange of free surface atoms and molecules with the surrounding environment [14,17,23,24] must be taken into account when considering the vacancy formation process. For most semiconductor materials, Frenkel pair formation is considered a less likely source of vacancies because of the higher energy of formation of two defects as a close pair. However, here, we focus only on the processes occurring in the AlAs volume. Therefore, we will neglect the formation and recombination of vacancies on the surface (Schottky defects) as well as the diffusion

of such defects from and to the surface. Thus, in the simple model under consideration, the vacancy concentration is determined by the temperature-activated formation of Frenkel pairs (vacancy + interstitial atom). In addition, we used the following approximations when building the model for simplification: (1) vacancies can be neutral or have different charge states, while the interstitial atom is neutral; (2) Frenkel pair recombination occurs only when the interstitial atom is in the nearest interstice to the vacancy (contact approximation); (3) neglect the participation of vacancies in the formation of complex defects, such as bivacancies and other point defect complexes.

In bulk crystal, the dynamics of vacancy formation can be described by the kinetic equation [13]:

$$\frac{\partial N_V(t)}{\partial t} = G(t) - R(t), \tag{1}$$

where N_V — the vacancy concentration, and G and R — the vacancy generation and recombination rates. The vacancy generation rate is described by the Arrhenius function $A\exp(-H_A/kT)$, where A — pre-exponential factor, H_A — enthalpy of Frenkel pair formation and k — Boltzmann constant. The factor A can be written in the form [13]:

$$A = \gamma_c N_{AP} N_{IP} \nu \exp\left[\frac{S_f + S_m}{k}\right], \tag{2}$$

where N_{AP} — the number of atoms capable of moving to an interstitial state to form a vacancy, N_{IP} — the number of interstitial states near the atoms N_{AP} (in a single volume crystal, we can consider $N_{AP} = N_{IP} = N$, where N — the density of atoms in the crystal lattice), ν — the Debye frequency, S_f and S_m — the formation and migration entropies, and γ_c — a coefficient depending on the mechanism of interaction between the vacancy and the interstitial atom. In our recent paper [13], it is shown that in the contact approximation $\gamma_c = a^3$, where a — is the lattice constant of the crystal. The enthalpy of Frenkel pair formation can be written as the sum of $H_A = H_f + H_m$, where H_f — the formation enthalpy and H_m — the migration enthalpy, which determines the breakdown of the tightly bound defect pair [14,25]. As a rule, the energy barrier for the migration of an interstitial atom is smaller than for a vacancy [26], so we will assume that H_m describes the interstitial atom migration.

The vacancy recombination rate can be written as [13]:

$$R = a^3 N_V N_I \nu \exp\left[\frac{S_m}{k}\right] \exp\left[-\frac{H_m}{kT}\right], \tag{3}$$

where N_I — the concentration of interstitial atoms.

For the formation of uncharged vacancies, V_{As}^0, we can write, using expressions (2) and (3), the rates of their generation and recombination in the following form:

$$G = N^2 G^0,$$

$$G^0 = a^3 \nu \exp\left[\frac{S_f + S_m}{kT}\right] \exp\left[-\frac{H_f^0 + H_m^0}{kT}\right], \tag{4a}$$

$$R = N_V N_i R^0, \quad R^0 = a^3 \nu \exp\left[\frac{S_m}{k}\right] \exp\left[-\frac{H_m}{kT}\right], \tag{4b}$$

where H_f^0 and H_m^0 — enthalpies of formation and migration of uncharged defects.

The solution of equation (1), taking into account expressions (4a) and (4b), gives, in thermodynamic equilibrium, the well-known expression for the equilibrium concentration of neutral vacancies formed by the Frenkel mechanism, which is independent of the state of the electronic subsystem of the crystal:

$$N_V^0 = N \exp\left[\frac{S_f}{2k}\right] \exp\left[-\frac{H_f}{2kT}\right]. \tag{5}$$

Let us now consider the generation rate during the formation of charged vacancies V_{As}^j in doped materials. During the formation of such vacancies, changes occur not only in the atomic but also in the electronic subsystems of the crystal [11,12,14,27,28]. The processes occurring in the electronic subsystem of the crystal influence the vacancy formation probability through changes in both the enthalpy of pair formation H_A and the pre-exponential factor A.

The vacancies formed in the anionic sublattice of compounds III–V are donors and can be in charge states 0, +1, +2 and +3 [29]. When a vacancy with positive charge j is born, due to the electroneutrality of the crystal, j electrons are added to the system. This results in a change in the formation enthalpy, which can be written as $H_A^j = H_A^0 + \Delta E_G^j$. The summand

$$\Delta E_G^j = \sum_{i=1}^{j} (E_{\mathrm{F}} - E_V^i),$$

where E_{F} — the position of the Fermi level and E_V^i — the energy of the electronic state in the band gap for a vacancy with charge i, describes the change in the energy of the electronic subsystem of the crystal at the birth of a charged vacancy.

The change in the energy of the electron subsystem at the birth of a singly charged vacancy is shown schematically in Fig. 1. It can be seen that ΔE_G^j depends on the doping level. As the Fermi level moves towards the valence band top, E_{vb}, it increases and, conversely, decreases as it moves towards the bottom of the conduction band, E_{cb}. All energies are counted from the valence band top E_{vb}, so the enthalpy of the charged vacancy activation increases ($\Delta E_G^{+1} > 0$) relative to the enthalpy of neutral vacancy activation at $E_{\mathrm{F}} > E_V^{+1}$ and, conversely, decreases ($\Delta E_G^{+1} < 0$) at $E_{\mathrm{F}} < E_V^{+1}$.

It should also be noted that the factor A must be corrected for the probability that there is j free space in the charged vacancy formation area to accommodate the released electrons. This probability is equal to the ratio of the hole concentration (p) to the density of valence band states (N_{vh}). Consequently, the number of the crystal lattice cells where a positively charged vacancy with charge j can be born is equal to $N(p/N_{vh})^j$.

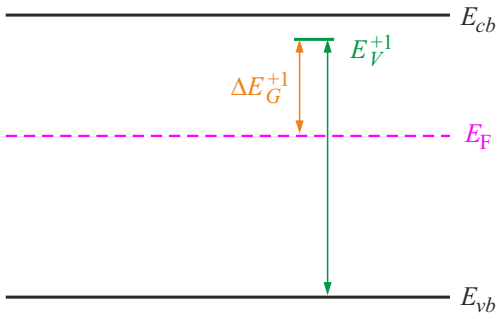

Figure 1. Schematic representation of the energy band diagram for a positively charged vacancy. Vertical arrows — the electron state energy of the vacancy in the band gap (E_V^{+1}) and the difference between the electron state energy of the vacancy and the position of the Fermi level (ΔE_g^{+1}).

For an non-degenerated semiconductor, when the condition $E_F - E_{vb} \leq kT$ is fulfilled, the hole concentration is described by the expression $p = N_{vh} \exp[-E_F/kT]$ [30], and the number of cells in which charged vacancies are born (and close to them interstitial states) is given by the expression $N_{AP} = N_{IP} = N(p/N_{vh})^j = N \exp[-jE_F/kT]$. Using this expression, we can write the generation rate for positively charge vacancies as:

$$G^j = N^2 \exp\left[-2j\frac{E_F}{kT}\right] G^0 \exp\left[-\frac{\sum_{i=1}^{j}(E_F - E_V^i)}{kT}\right]. \quad (6)$$

At the same time, the recombination rate of charged vacancies involving a neutral interstitial atom does not depend on the electron subsystem state and is described by the expression (4b).

Vacancies forming in different charge states can be recharged after their birth. Therefore, the dynamics of vacancy concentration in different charge states is described by a system of kinetic equations taking into account their recharging:

$$\frac{\partial N_V^0(t)}{\partial t} = N^2 G^0 - N_V^0(t) N_I(t) R^0 + \sum_{i=1}^{3}\left(\gamma^i\left(N_V^{+i}(t)\exp\left[-\frac{E_V^{+i} - E_F(t)}{kT}\right] - N_V^0(t)\right)\right), \quad (7)$$

$$\frac{\partial V_V^{+1}(t)}{\partial t} = N^2 G^0 \exp\left[\frac{E_V^{+1} - 3E_F(t)}{kT}\right] - N_V^{+1}(t) N_I(t) R^0 + \gamma^1 N_V^0(t) - \gamma^1 N_V^{+1}(t)\exp\left[-\frac{E_V^{+1} - E_F(t)}{kT}\right],$$

$$\frac{\partial N_V^{+2}(t)}{\partial t} = N^2 G^0 \exp\left[\frac{\sum_{i=1}^{2}(E_V^i - E_F(t)) - 4E_F(t)}{kT}\right] - N_V^{+2}(t) N_I(t) R^0 + \gamma^2 N_V^0(t) - \gamma^2 N_V^{+2}(t)\exp\left[-\frac{E_V^{+2} - E_F(t)}{kT}\right],$$

$$\frac{\partial N_V^{+3}(t)}{\partial t} = N^2 G^0 \exp\left[\frac{\sum_{i=1}^{3}(E_V^i - E_F(t)) - 6E_F(t)}{kT}\right] - N_V^{+2}(t) N_I(t) R^0 + \gamma^3 N_V^0(t) - \gamma^3 N_V^{+3}(t)\exp\left[-\frac{E_V^{+3} - E_F(t)}{kT}\right],$$

$$N_I(t) = N_V^0(t) + N_V^{+1}(t) + N_V^{+2}(t) + N_V^{+3}(t),$$

$$N_{ec}\exp\left[\frac{E_F(t) - E_{cb}}{kT}\right] - N_{vh}\exp\left[-\frac{E_F(t)}{kT}\right] - N_V^{+1}(t) - N_V^{+2}(t) - N_V^{+3}(t) - N_D + N_A = 0.$$

The first four equations, where γ^i — emission coefficient i electrons with neutral vacancy, describe the vacancy recharge dynamics. The fifth equation reflects the equality of the concentrations of interstitial atoms and vacancies born as Frenkel pairs. Finally, the electroneutrality equation, where N_A and N_D — the concentrations of acceptors and donors, describes the change in the balance of the concentration of free charge carriers during the formation of charged vacancies. It should be noted that we consider the high-temperature approximation of a weakly compensated ($N_A \ll N_D$ or $N_D \ll N_A$) wide-band crystal when all dopant impurities are ionized and the concentration of intrinsic electrons and holes is much smaller than the doping impurity concentration.

To calculate the dynamics of vacancy formation, we used the AlAs parameters taken from [31], the enthalpy of neutral vacancy formation in the arsenic sublattice $H_f^0 = 3.83$ eV [32], the enthalpy of interstitial atom migration $H_m^0 = 2.7$ eV, and the energies of electronic levels in the band gap of AlAs for arsenic vacancies in different charge states: $E_V^{+1} = 0.94 \cdot E_g$, $E_V^{+2} = 0.20 \cdot E_g$ and $E_V^{+3} = 0.06 \cdot E_g$, where E_g — the band gap width of AlAs [29], and the Debye frequency $\nu = 1.3 \cdot 10^{13}$ Hz [33]. Since the values of the parameters S_f and S_m are determined mainly by the configuration entropy [14], we have taken the values of these parameters determined for a GaAs — crystal, with a lattice configuration the same as that of the AlAs [34,35]. The calculation results are shown in Fig. 2, *a* and *b*.

The vacancy concentration dynamics in all charge states presents a typical increasing curve with saturation.

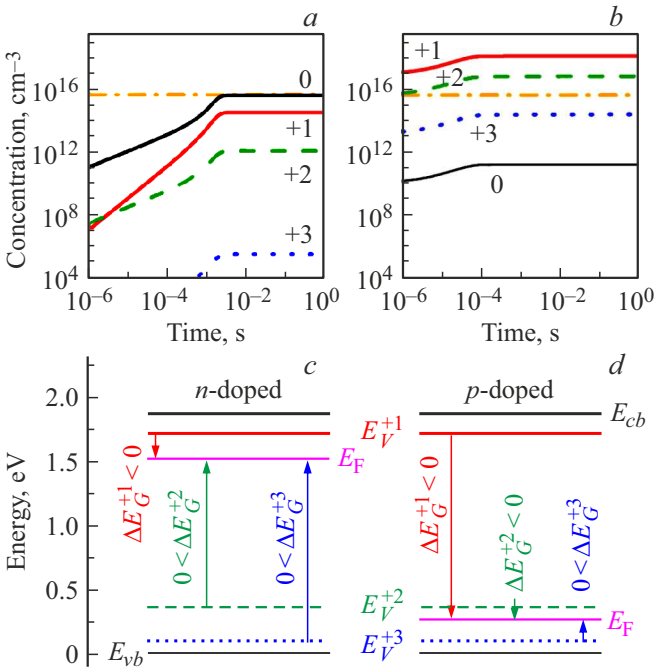

Figure 2. Vacancy concentration dynamics in different charge states at 1100 K: *a* — in *n*-doped and *b* — in *p*-doped AlAs. The horizontal dashed line indicates the equilibrium concentration of neutral vacancies calculated from formula (5). The energy states of charged vacancies, the position of the Fermi level, and the energy change of the electronic subsystem of the crystal at the birth of vacancies in different charge states: *c* — in *n*-doped and *d* — in *p*-doped material. (A color version of the figure is provided in the online version of the paper).

In *n*-doped AlAs, as seen in Fig. 2, *a*, mainly uncharged arsenic vacancies are formed, and their concentration saturates, reaching an equilibrium value. The concentration of charged vacancies is noticeably smaller and consistently decreases with increasing positive charge $N_V^{+1} > N_V^{+2} > N_V^{+3}$. In *p*-doped AlAs (Fig. 2, *b*), the formation of singly charged vacancies becomes the most efficient process, with their concentration being 2 order of magnitude greater than the equilibrium concentration of neutral vacancies. The concentrations of vacancies in other charge states are markedly lower, and their ratio is determined by the $N_V^{+2} > N_V^{+3} > N_V^0$ sequence.

The efficiency of formation of vacancies located in different charge states is determined, as can be seen from expression (6), by the formation enthalpy and the fraction of crystal lattice cell, where vacancy formation is possible. In *n*-doped material, as seen in Fig. 2, *c*, the $N_V^0 > N_V^{+2} > N_V^{+3}$ relation is fulfilled because the enthalpy of vacancy formation in the charge states V_{As}^{+2} and V_{As}^{+3} is larger than that in the V_{As}^0 state. At the same time, a small decrease in the enthalpy of vacancy formation in the state V_{As}^{+1} (as compared to V_{As}^0) is compensated by the low concentration of crystal lattice cell, where the formation of positively charged vacancies is possible, which ensures the dominance of neutral $N_V^0 > N_V^{+1}$ vacancies. On the other hand, in the *p*-doped material, as can be seen from Fig. 2, *d*, there is a significant (comparable to the band gap width of AlAs) decrease in the formation enthalpy for vacancies in the state of V_{As}^{+1}, which leads to the dominance of such vacancies in this material. It should also be noted that the ratio of concentrations $N_V^{+2} > N_V^{+3} > N_V^0$ in *p*-doped AlAs does not reflect the ratio of the probabilities of vacancy formation in these charge states. Obviously, the formation enthalpy is lower for V_{As}^0 (Fig. 2, *d*), and the fraction of lattice cells, where their formation is possible, is higher than that for vacancies in the V_{As}^{+3} state. The observed concentration ratio is due to the recharging of vacancies already after their formation.

2.2. High-temperature annealing of doped Al(Sb,As)/AlAs-heterostructures: diffusion of antimony into AlAs

Since the diffusion of substitutional impurities in AlAs proceeds by the vacancy mechanism, the diffusion constant of such impurity (D) can be written as $D = D_V N_V / N$, where D_V and N_V — the diffusion constant and the total concentration of vacancies [36]. Thus, a change in the formation rate of charged vacancies at a change in the concentration of charge carriers should lead, other things being equal, to a change in the diffusion rate of substitutional impurities in this material.

To validate the modelling results, we performed an experimental study of antimony diffusion in the anionic sublattice of heterostructures with Al(Sb,As)/AlAs quantum dots. The heterostructures were grown by molecular-beam epitaxy on semi-insulating GaAs orientation (001) substrates. The structures contained a single layer of QD placed between the AlAs layers. The density ($5 \cdot 10^{10}$ cm $^{-2}$) and mean diameter (20 nm) of the QDs were determined by electron microscopy in [37]. The relatively low dot density prevents the redistribution of charge carriers across the ensemble of QD [38,39]. A GaAs cover layer was grown to protect the top AlAs layer from oxidation. The concentration of charge carriers in the heterostructure was changed by doping it with a donor (silicon) or acceptor (beryllium) impurity to the level of $5 \cdot 10^{18}$ cm^{-3}. The technology of growing heterostructures is described in detail in [37,40,41]. To prevent As sublimation from the surface of the structures at high temperatures, the structures were coated with a protective layer of SiO_2 with a thickness of 150 nm [5].

Antimony diffusion was stimulated by high-temperature annealing in an H_2 flux for 10 min in the temperature range 600–850°C. The material mixing degree was analyzed by the shift of the exciton recombination band position, in the photoluminescence (PL) spectra of the structures measured at liquid nitrogen temperature. The PL was excited by a semiconductor laser ($h\nu = 3.06$ eV) and measured at a unit based on an Acton Advanced SP500A spectrograph equipped with a cooled CCD camera.

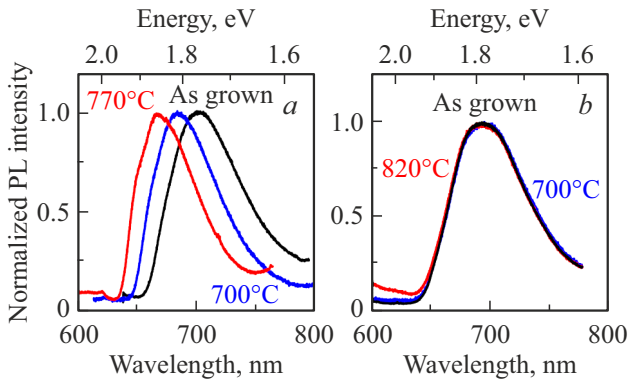

Figure 3. Photoluminescence spectra of heterostructures with Al(Sb,As)/AlAs quantum dots annealed at different temperatures: *a* — structures doped with acceptors; *b* — structures doped with donors.

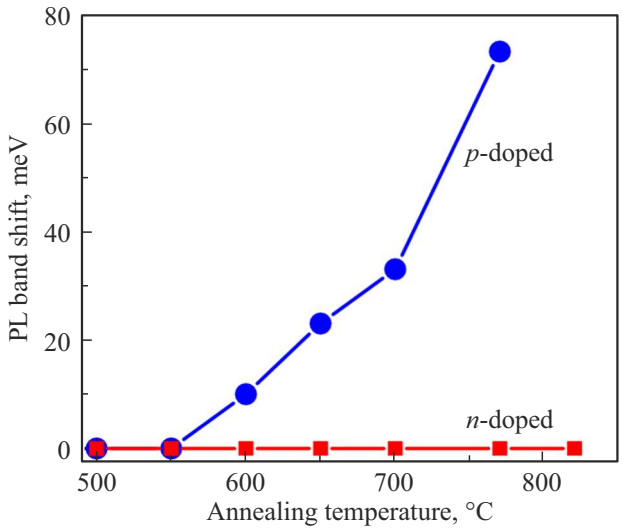

Figure 4. Blue shift of the position of the emission band maximum in the photoluminescence spectra of *n*- and *p*-doped heterostructures with Al(Sb,As)/AlAs quantum dots, as a function of annealing temperature.

The normalized PL spectra of heterostructures with Al(Sb,As)/AlAs QDs are shown in Fig. 3, *a* and *b*. The PL bands in the spectra of the non-annealed (as grown) structures are shown by black curves and have a maximum of 1.767 and 1.792 eV, respectively, for *p*- and *n*-doped structures. The width of the bands is due to the variation in the QD size and the solid solution composition from which the QDs are formed.

Ten-minute annealing at temperatures 550°C and below has no effect on the shape of the PL spectra. When the annealing temperature is increased to 600°C, a band shift to the short-wavelength area of the spectrum (blue shift) is observed in the PL spectra of *p*-doped heterostructures. The blue shift increases with increasing annealing temperature as shown in Fig. 4. At the same time, increasing the annealing temperature up to 820°C has no effect on the band position in the PL spectra of *n*-doped heterostructures (see Fig. 3, *b* and 4).

The blue shift of the bands in the PL spectra of heterostructures after high-temperature annealing is caused by the change in the band gap width of the Al(Sb,As)/AlAs QD because of the increase in the AlAs proportion in the solid solution AlSbAs [5], due to the antimony diffusion into AlAs. Thus, the experimental results indicate that an increase in the hole concentration promotes an increase in the rate of generation of charged arsenic vacancies in the anionic sublattice of AlAs and thus an increase in the antimony diffusion constant described by the expression:

$$D = \frac{D_V}{N} \sum_{i=0}^{3} N_V^i.$$

3. Conclusion

The influence of charge carriers concentration on the formation of vacancies by the Frenkel mechanism in the anionic sublattice of AlAs has been investigated. In *n*-doped material, the concentration of these defects is determined by the formation of neutral vacancies, the probability of formation of which does not depend on the concentration of charge carriers. In the transition to *p*-doped material, the probability of formation of positively charged vacancies increases and, starting from some doping level, the total concentration of vacancies starts to exceed the equilibrium concentration of neutral vacancies. An increase in the vacancy concentration leads to an increase in the diffusion rate of substitutional impurities. The increase in the vacancy-stimulated diffusion constant of antimony at high temperatures with increasing hole concentration has been experimentally demonstrated in heterostructures with Al(Sb,As)/AlAs quantum dots.

Funding

This study was financially supported by the Russian Science Foundation (project No. 22-12-00022).

Conflict of interest

The authors declare that they have no conflict of interest.

References

[1] Richard J.D. Tilley. *Defects in solids* (John Wiley & Sons, Ltd, 2008).
[2] *Diffusion Processes in Advanced Technological Materials* edited by Devendra Gupta (Springer Verlag, N.Y., 2005).
[3] B. Tuck. J. Phys. D: Appl. Phys., **18**, 557 (1985).
[4] Shambhu Sharan Kumar Sinha, Subindu Kumar, Mukul Kumar Das. Appl. Phys. A, **125**, 774 (2019).
[5] T.S. Shamirzaev, A.K. Kalagin, A.I. Toropov, A.K. Gutakovskii, K.S. Zhuravlev, Phys. Status Solidi C, **3** (11), 3932 (2006).

[6] M.Yu. Petrov, I.V. Ignatiev, S.V. Poltavtsev, A. Greilich, A. Bauschulte, D.R. Yakovlev, M. Bayer. Phys. Rev. B, **78**, 045315 (2008).
[7] S.O. Hruszkewycz, S. Maddali, C.P. Anderson, W. Cha, K.C. Miao, M.J. Highland, A. Ulvestad, D.D. Awschalom, F.J. Heremans. Phys. Rev. Mater., **2**, 086001 (2018).
[8] T.S. Shamirzaev. FTP, **45**, 97 (2011). (in Russian).
[9] D.S. Abramkin, T.S. Shamirzaev. Fiz. Tekh. Poluprovodn., **53**, 710 (2019). (in Russian).
[10] T.S. Shamirzaev, J. Debus, D.S. Abramkin, D. Dunker, D.R. Yakovlev, D.V. Dmitriev, A.K. Gutakovskii, L.S. Braginsky, K.S. Zhuravlev, M. Bayer. Phys. Rev. B, **84**, 155318 (2011).
[11] E.G. Seebauer, M.C. Kratzer. Mater. Sci. Eng. R, **55**, 57 (2006).
[12] V.L. Vinetsky, G.A. Kholodar. *Statisticheskoye vzaimodeystviye elektronov i defektov v poluprovodnikakh* (Kiev, Nauk. Dumka, 1969). (In Russian)
[13] T.S. Shamirzaev, V.V. Atuchin, V.E. Zhilitskiy, A.Y. Gornov. Nanomaterials, **13**, 308 (2023).
[14] C. Freysoldt, B. Grabowski, T. Hickel, J. Neugebauer. Rev. Mod. Phys., **86**, 253 (2014).
[15] J. Gebauer, M. Lausmann, F. Redmann, R. Krause-Rehberg, H.S. Leipner, E.R. Weber, P. Ebert. Phys. Rev. B, **67**, 235207 (2003).
[16] H.S. Djie, O. Gunawan, D.-N. Wang, B.S. Ooi, J.C.M. Hwang. Phys. Rev. B, **73**, 155324 (2006).
[17] J-L. Rouviere, Y. Kim, J. Cunningham, J.A. Rentschler, A. Bourret, A. Ourmazd. Phys. Rev. Lett., **68**, 2798 (1992).
[18] M. Feiginov J. Infrared Millim. Terahertz Waves, **40**, 365 (2019).
[19] Saad Muttlak, Omar Abdulwahid, James Sexton, Michael J. Kelly, M. Missous. IEEE J. Electron Dev. Soc., **6**, 254 (2018).
[20] Y. Alahmadi, W.P. LiKam. Semicond. Sci. Technol., **34**, 025010 (2019).
[21] P. Lever, H.H. Tan, C. Jagadish. J. Appl. Phys., **96**, 7544 (2004).
[22] I. McKerracher, L. Fu, H.H. Tan, C. Jagadish. J. Appl. Phys., **112**, 113511 (2012).
[23] D.T.J. Hurle. J. Appl. Phys., **85**, 6957 (1999).
[24] T.S. Shamirzaev, A.L. Sokolov, K.S. Zhuravlev, A.Yu. Kobitski, H.P. Wagner, D.R.T. Zahn. Fiz. Tekh. Poluprovodn., **36**, 87 (2002). (in Russian).
[25] J.H. Crawford, jr., L.M. Slifkin (eds). *Point defects in solids. In Semiconductors and Molecular Crystals* (Plenum Press, N.Y., USA, 1975) v. 2.
[26] A.F. Wright, N.A. Modine. J. Appl. Phys., **120**, 215705 (2016).
[27] G.A. Baraff, M. Schliiter. Phys. Rev. Lett., **55**, 1327 (1985).
[28] W. Walukiewicz. Appl. Phys. Lett., **54**, 2094 (1989).
[29] M.J. Puska. J. Phys.: Condens. Matter., **1**, 7347 (1989).
[30] M. Grundmann. *The Physics of Semiconductors* (Springer Verlag, Berlin–Heidelberg, Germany, 2006).
[31] I. Vurgaftman, J.R. Meyer, L.R. Ram-Mohan. J. Appl. Phys., **89**, 5815 (2001).
[32] H.A. Tahini, A. Chroneos, S. Murphy, U. Schwingenschlogl, R.W. Grimes. J. Appl. Phys., **114**, 063517 (2013).
[33] B. Ullrich, M. Bhowmick, H. Xi. AIP Advances, **7**, 045109 (2017).
[34] P. Mitev, S. Seshadri, L.J. Guido, D.T. Schaafsma, D.H. Christensen. Appl. Phys. Lett., **73**, 3718 (1998).
[35] M. Bockstedte, M. Schefer. Z. Phys. Chem., **200**, 195, (1997).
[36] O.M. Khreis, W.P. Gillin, K.P. Homewood. Phys. Rev. B, **55**, 15813 (1997).
[37] D.S. Abramkin, K.M. Rumenin, A.K. Bakarov, D.A. Kolotovkina, A.K. Gutakovsky, T.S. Shamirzaev. Pis'ma ZHETF, **103** (11), 785 (2016).
[38] T.S. Shamirzaev, D.S. Abramkin, D.V. Dmitriev, A.K. Gutakovskii. Appl. Phys. Lett., **97**, 263102 (2010).
[39] T.S. Shamirzaev, A.M. Gilinsky, A.K. Kalagin, A.I. Toropov, A.K. Gutakovskii, K.S. Zhuravlev. Semicond. Sci. Technol., **21**, 527 (2006).
[40] T.S. Shamirzaev, D.R. Yakovlev, N.E. Kopteva, D. Kudlacik, M.M. Glazov, A.G. Krechetov, A.K. Gutakovskii, M. Bayer. Phys. Rev. B, **106**, 075407 (2022).
[41] T.S. Shamirzaev, D.R. Yakovlev, A.K. Bakarov, N.E. Kopteva, D. Kudlacik, A.K. Gutakovskii, M. Bayer. Phys. Rev. B, **102**, 165423 (2020).

Translated by Y.Deineka